Deep-Water Formation in the North Pacific During the Late Miocene Global Cooling

Lina Zhai, Shiming Wan, Christophe Colin, Debo Zhao, Yuntao Ye, Zhaojun Song, Xuebo Yin, Xuefa Shi, Anchun Li

Paleoceanography and Paleoclimatology

RESEARCH ARTICLE
10.1029/2020PA003946

Special Section:
The Miocene: The Future of the Past

Deep-Water Formation in the North Pacific During the Late Miocene Global Cooling

Lina Zhai[1,2], Shiming Wan[1,3,4], Christophe Colin[5], Debo Zhao[1], Yuntao Ye[6], Zhaojun Song[7], Xuebo Yin[1], Xuefa Shi[8], and Anchun Li[1]

[1]Key Laboratory of Marine Geology and Environment, Institute of Oceanology, Chinese Academy of Sciences, Qingdao, China, [2]Center for Ocean Mega-Science, Chinese Academy of Sciences, Qingdao, China, [3]Laboratory for Marine Geology, Qingdao National Laboratory for Marine Science and Technology, Qingdao, China, [4]CAS Center for Excellence in Quaternary Science and Global Change, Xi'an, China, [5]Laboratoire GEOsciences Paris-Sud (GEOPS), UMR 8148, CNRS-Université de Paris-Sud, Université Paris-Saclay, Orsay, France, [6]Key Laboratory of Petroleum Geochemistry, Research Institute of Petroleum Exploration and Development, China National Petroleum Corporation, Beijing, China, [7]College of Earth Science and Engineering, Shandong University of Science and Technology, Qingdao, China, [8]Key Laboratory of Marine Sedimentology and Environmental Geology, First Institute of Oceanography, Ministry of Natural Resources, Qingdao, China

Abstract A multiproxy study including organic carbon and bulk nitrogen isotopes along with major and trace element concentrations in sediments from Integrated Ocean Drilling Program (IODP) Sites U1425 and U1430 in the Japan Sea have been conducted in order to trace deep-water evolution in the Japan Sea and the North Pacific since the late Miocene. The high total organic carbon (TOC) flux, as well as other published geochemical and sedimentary evidence, indicates the occurrence of anoxic deep-water in the Japan Sea before ~7.4 Ma. The low-nitrogen isotope values probably suggest nearly complete denitrification. In contrast, the sharply enhanced biological production but decreased burial of organic matter during ~7.4–4 Ma, as shown by high enrichment factor of Ba (Ba_{EF}) values, together with low TOC flux, highlights enhanced deep-water oxygenation in the Japan Sea during that time. We suggest that deep-water formation in the North Pacific ventilated the deep Japan Sea via northern deep seaways before the sea became semi-closed in the early Pliocene. The synchronously increased equator-to-pole temperature gradients driven by late Miocene global cooling may have caused southward shift of mid-latitude storm tracks, coupled with the weakened East Asian summer monsoon and moisture transport, leading to decreased precipitation in mid-latitude regions. The potential increases in surface salinity in the North Pacific may have broken the ocean stratification and favored deep-water formation, and further caused deep-water ventilation in the Japan Sea.

Plain Language Summary Deep-water formation plays a significant role in deep ocean ventilation in the modern North Atlantic and South Ocean, while absent in the North Pacific. Whether deep-water formation occurred in the North Pacific in the late Miocene global cooling remains unknown. The Japan Sea is an ideal place to test this phenomenon since it had deep-water exchange with the North Pacific during the late Miocene-early Pliocene. We analyze the organic carbon and bulk nitrogen isotopes and major and trace element concentrations of sediments since 11 Ma from IODP Sites U1425 and U1430 in the Japan Sea. During ~7.4–4 Ma, the enhanced biological production along with decreased organic carbon burial indicates enhanced deep-water oxygenation in the Japan Sea. We attribute this to potential deep-water formation in the North Pacific, which was probably caused by weakened precipitation in mid-latitude regions of the Northern Hemisphere and the resultant increased surface salinity in the North Pacific during the late Miocene cooling.

Key Points:
- Paleoproductivity and paleoredox evolution in the Japan Sea since 11 Ma was reconstructed
- Low-organic burial efficiency was caused by deep-ocean oxygenation during ~7.4–4 Ma
- Deep-water formed in the North Pacific ventilated the deep Japan Sea during the late Miocene-early Pliocene

Supporting Information:
- Supporting Information S1

Correspondence to:
S. Wan,
wanshiming@ms.qdio.ac.cn

Citation:
Zhai, L., Wan, S., Colin, C., Zhao, D., Ye, Y., Song, Z., et al. (2021). Deep-water formation in the North Pacific during the late Miocene global cooling. *Paleoceanography and Paleoclimatology*, *36*, e2020PA003946. https://doi.org/10.1029/2020PA003946

Received 8 APR 2020
Accepted 27 JAN 2021

1. Introduction

Intermediate-deep layers are well-ventilated in most modern oceans (Figure 1a), typically in the North Atlantic and Southern Oceans; this is primarily related to deep-water formation (Marshall & Speer, 2012; Weaver et al., 1999). This process plays a fundamental role in regulating global climate by affecting heat, gas exchange and nutrient cycles (Burls et al., 2017). In contrast, no new deep-water mass are formed in the modern North Pacific due to low-surface salinities and the existence of a strong halocline (Emile-Geay

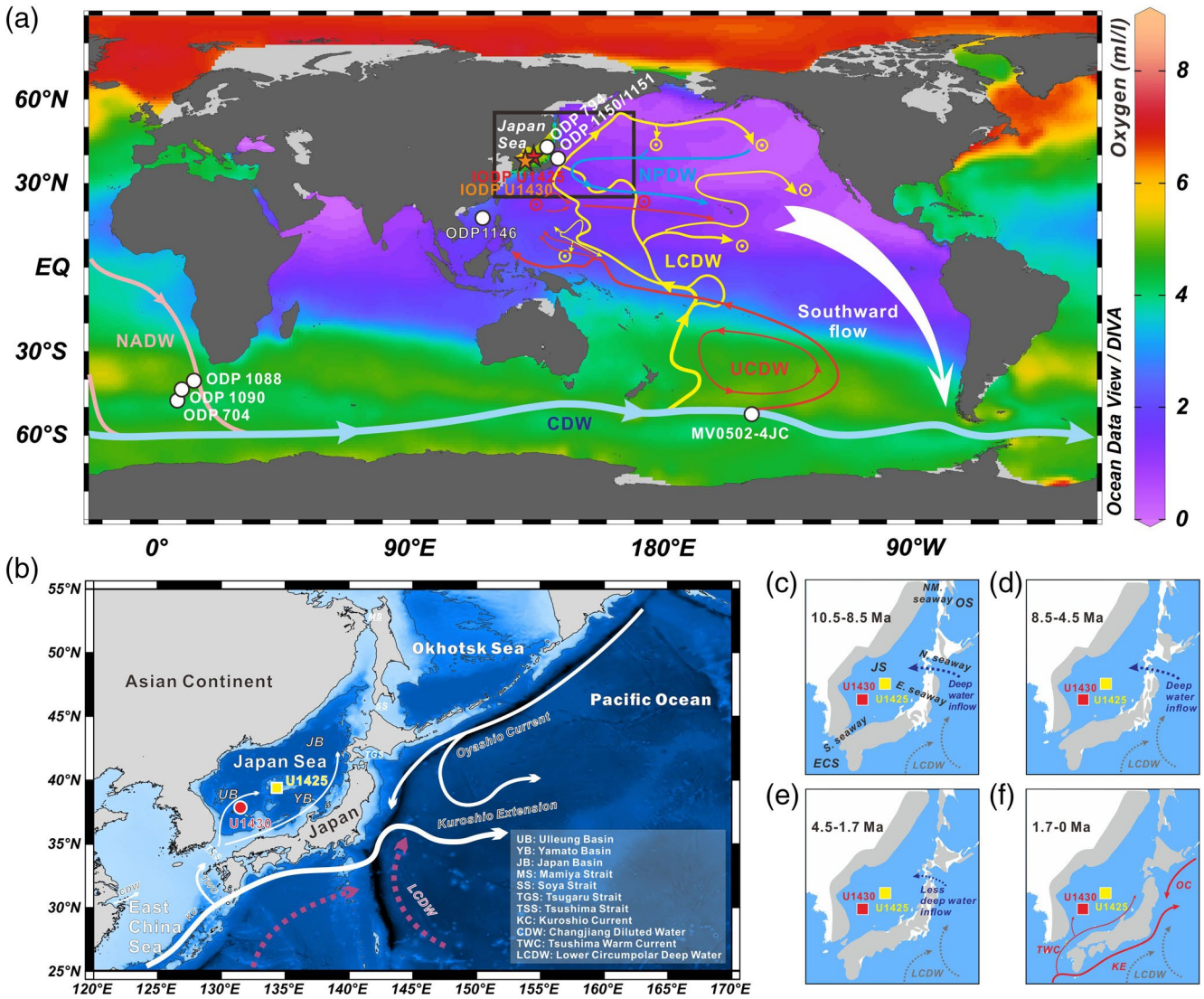

Figure 1. (a) Modern oxygen concentration distribution at 1,000 m in global oceans along with modern deep Pacific Ocean circulation (modified from Kawabe & Fujio, 2010); also shown are the locations of IODP Sites U1425 and U1430 in the Japan Sea and other sites referred in this study. Yellow and red circles with a central point represent upwelling of Lower Circumpolar Deep Water (LCDW) and Upper Circumpolar Deep Water (UCDW), respectively. The white arrow shows the flow carrying modified North Pacific Deep Water (NPDW) to mix with UCDW. NADW, North Atlantic Deep Water. (b) Local oceanographic setting of the Japan Sea. Surface and deep circulations are indicated by white solid and red dotted arrows, respectively. (c–f) Schematic diagram showing paleoceanographic evolution of the Japan Sea since 10.5 Ma (modified from Kozaka et al., 2018). The blue dotted arrow indicates the northern deep seaway (>1,000 m) allowing NPDW and LCDW (black dotted arrows) to enter the Japan Sea during ~10.5–4.5 Ma. The red arrows indicate modern surface current. The land around the Japan Sea is shown by gray shading. E. seaway, eastern seaway; ECS, East China Sea; IODP, Integrated Ocean Drilling Program; JS, Japan Sea; KE, Kuroshio Extension; N. seaway, northern seaway; NM. seaway, northernmost seaway; OC, Oyashio Current; OS, Okhotsk Sea; S. seaway, southern seaway; TWC, Tsushima Warm Current.

et al., 2003; Ferreira et al., 2018; Warren, 1983). It has been proposed that deep-water, formed due to increased surface salinity driven by subdued freshwater flux during the last deglacial cold events, may have played a key role in global heat distribution and carbon cycles (Okazaki et al., 2010; Rae et al., 2014, 2020; Yu et al., 2020). However, some studies argue that during the deglacial cold events, only enhanced intermediate-water ventilation occurred above a depth of ~2,000 m in the North Pacific driven by the active polynya formation and brine rejection during sea ice formation in the Okhotsk Sea and/or western Bering Sea, while the deep ocean remained isolated (Gong et al., 2019; Jaccard & Galbraith, 2013; Max et al., 2014; Ohkushi et al., 2003). Other than the intermediate-deep ocean ventilation during cold events, a recent model work

suggested that deep-water formation could occur in the North Pacific during the warm Pliocene, in response to decreased precipitation over the mid-latitudes driven by the reduced meridional sea surface temperature (SST) gradients at that time (Burls et al., 2017), although stronger density stratification is generally expected to be formed under global warming (Jenkyns, 2003, 2010; Sarmiento et al., 1998). Such inconsistencies will impede our understanding of the precise role of deep-water formation in the North Pacific in the global climate change, and further cause difficulty in future climate projection.

The late Miocene (~7–5.4 Ma) is marked by prolonged global cooling revealed by declines in global ocean temperature (Herbert et al., 2016), which are largely concurrent with remarkable environmental and ecosystem changes, involving carbon-isotopic shift and "biogenic bloom" in global oceans (Dickens & Owen, 1999; Diester-Haass et al., 2006), as well as aridification and vegetation shifts on land (Cerling et al., 1997; Holbourn et al., 2018). The climate change could exert significant influences on atmosphere-ocean circulation (Holbourn et al., 2018; Matsuzaki et al., 2020), which probably resulted in specific patterns of deep-water circulation in the North Pacific that differ from the modern conditions. However, to date, little is known about the potential impact of climate change on deep-water circulation patterns in the North Pacific due to a lack of successive, well-dated, representative records.

The Japan Sea is a semi-closed marginal basin located along the eastern edge of the Eurasian continent and NW of the Pacific plates; the only intrusion is of surface water, known as the Tsushima Warm Current (TWC), and it produces oxygen-rich deep-water by cooling in the northwest of the sea in winter (Gamo et al., 2014; Figure 1b). Unlike the modern restricted Japan Sea, sustained deep-water intrusion into the Japan Sea from the North Pacific occurred during the late Miocene-early Pliocene, identified by the existence of radiolarian species related to the North Pacific deep-water and seawater Nd isotope reconstruction in the Japan Sea (S. Kamikuri and Motoyama, 2007; Kozaka et al., 2018; Tada, 1994; Figures 1c–1f). Sedimentological and geochemical data suggested that oxygen-deficient bottom water prevailed in the Japan Sea during the late Miocene (Hanagata, 2003; Tada, 1994; Yamamoto et al., 2005). Therefore, sediments in the Japan Sea provide an opportunity to track the evolution of deep-water circulation in the North Pacific during the late Miocene-early Pliocene. Here, we present organic carbon and bulk nitrogen isotopic compositions ($\delta^{13}C_{org}$ and $\delta^{15}N_{bulk}$), and an elemental proxy (Ba_{EF}) for marine productivity reconstruction in the sediments from Integrated Ocean Drilling Program (IODP) Sites U1425 and U1430. The aim is to trace deep-water ventilation in the Japan Sea based on changes in paleoproductivity and redox conditions since 11 Ma, and to determine the roles of local tectonic activity, sea level changes and deep-water evolution in the North Pacific in deep-water oxygenation of the Japan Sea.

2. Geological and Oceanographic Setting of the Japan Sea

The Japan Sea is composed of three major basins, the Japan Basin, the Yamato Basin and the Ulleung Basin (Figure 1b), which were developed by continental rifting and seafloor spreading during the early Oligocene (~32 Ma) to middle Miocene (~15 Ma) and subsequent regional subsidence (Jolivet et al., 1994; Tada et al., 2015; Tamaki et al., 1992). The northern Japanese islands were fragmented and largely submerged as a bathyal environment since the beginning of the late Miocene (~10 Ma) until the Pliocene, while the southern parts were landmass connected to the Korean Peninsula during ~10 to 3.5 Ma (Iijima & Tada, 1990; Itaki, 2016; Kozaka et al., 2018).

At present, the Japan Sea is connected to its neighboring seas only through four shallow and narrow straits: the East China Sea through the Tsushima Strait (sill depth at ~130 m), the Okhotsk Sea through the Mamiya Strait (~18 m) and Soya Strait (~55 m), and the western North Pacific through the Tsugaru Strait (~130 m). The TWC, a branch of the Kuroshio Current, is the only current flowing into the Japan Sea through the Tsushima Strait (Figure 1b). However, the paleoceanographic conditions of the Japan Sea have changed dramatically since the Miocene (Tada, 1994). The Japan Sea had deep-water connection with the North Pacific via the northern seaways during the late Miocene to the early Pliocene (S. Kamikuri and Motoyama, 2007; Kozaka et al., 2018; Matsuzaki et al., 2018; Tada, 1994). Notably, the significant intrusion of the TWC via the Tsushima Strait began at ~1.7 Ma, which was likely related to the stretching of the Okinawa Trough since ~2 Ma (Gallagher et al., 2015; Gungor et al., 2012; Itaki, 2016; Shinjo, 1999). Since then,

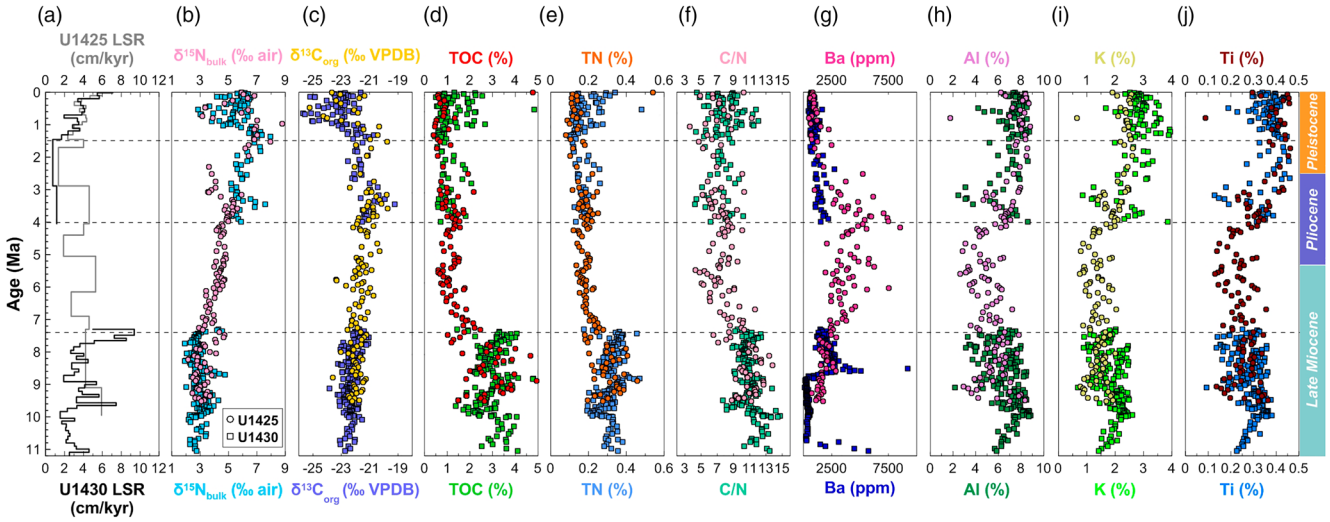

Figure 2. Variations of (a) linear sedimentation rates (LSR), (b) $\delta^{15}N_{bulk}$, (c) $\delta^{13}C_{org}$, (d) TOC, (e) TN, (f) C/N (atomic ratio), (g) Ba, (h) Al, (i) K, and (j) Ti at IODP Sites U1425 and U1430 since 11 Ma. IODP, Integrated Ocean Drilling Program; TN, total nitrogen; TOC, total organic carbon.

the paleoceanographic conditions of the Japan Sea were largely controlled by periodical sea level changes and flux of the TWC (Tada et al., 1999).

3. Materials and Methods

IODP Site U1425 (39°29.44′ N, 134°26.55′ E, 1909 m water depth) is situated on a terrace in a north-east-southwest-oriented graben in the middle of the Yamato Bank. IODP Site U1430 (37° 54.16′ N, 131° 32.25′ E, 1,072 m water depth) is located on the southern upper slope of the eastern South Korea Plateau (Figure 1b). The two sites show similar sedimentary successions, dominated by clayey silt, silty clay, nannofossil ooze, diatom ooze, claystone, and sandstone (Tada et al., 2015). The sediments at Site U1425 were deposited continuously, with basically constant sedimentation rates of 3.9 cm/kyr since 9.5 Ma (Figure 2). In contrast, the sedimentation rates at Site U1430 varied greatly and a sediment hiatus occurred in the period ~7.3–4 Ma (Matsuzaki et al., 2018; Tada et al., 2015). This hiatus coincides in depth with a regional unconformity on seismic profiles (MB3 unconformity) extending over much of the eastern South Korea Plateau (Horozal et al., 2017). Although the cause is uncertain, it may be attributed to erosion by bottom currents or a brief episode of local tectonic uplift (Horozal et al., 2017; Kurokawa et al., 2019). Age models of the sediments from Sites U1425 and U1430 were established on the basis of magnetostratigraphy and biostratigraphy (S. I. Kamikuri et al., 2017; Tada et al., 2015) combined with a revised age model for the Pleistocene (Tada et al., 2018).

For this study, we focus on composite depth samples of the upper 357 m (after 9.5 Ma) at Site U1425 and the upper 208 m (after 11 Ma) at Site U1430. A total of 403 samples (137 samples from Site U1425 and 266 samples from Site U1430) were investigated for geochemical analyses of $\delta^{13}C_{org}$ and $\delta^{15}N_{bulk}$, as well as major and trace element concentrations. We combined previously published major and trace elements and TOC results from Site U1430 since 4 Ma (Zhai et al., 2020) and the new elemental concentrations and isotopic data to reconstruct the evolution of paleoenvironment and paleoproductivity in the Japan Sea since the late Miocene.

For major and trace element analyses, ~40 mg of dried and powdered material from each sample was mixed with acids (1.5 mL HF + 0.5 mL HNO_3) in a Teflon beaker and kept on a hot plate at 150°C for 24 h. Then, 0.5 mL $HClO_4$ was added to the open beaker and heated on a hot plate to dryness at 150°C. After the addition of 1 mL HNO_3 and 1 mL H_2O in a sealed beaker for 12 h, the solution was diluted with 40 g of deionized water. The major and trace element concentrations were measured at the Institute of Oceanology, Chinese Academy of Sciences (IOCAS), Qingdao, using a Thermo Icap6300 ICP-AES and a Perkin-Elmer

ELAN DRC II ICP-MS, respectively (Wan et al., 2015). The analytical precision (relative standard deviation [RSD]) is generally better than 1% for major elements and 3% for trace elements. Elemental enrichment factors (EFs) were calculated to evaluate the degree of authigenic enrichment (Tribovillard et al., 2006): $X_{EF} = (X/Al)_{sample}/(X/Al)_{PAAS}$, where X and Al represent the weight concentrations of elements X and Al, respectively. Samples were normalized using the PostArchean Australian Shale (PAAS) compositions (Taylor & Mclennan, 1985). Enrichment factor of Ba (Ba_{EF}) is used as a good indicator of paleoproductivity and has the advantage of being relatively stable in oxic and/or anoxic waters (Schoepfer et al., 2015), although it is preferentially lost in sulfate-depleted anoxic waters (Schenau et al., 2001).

The determinations of total organic carbon (TOC) and total nitrogen (TN) concentrations and isotopic composition were carried out at the Yantai Institute of Coastal Zone Research, Chinese Academy of Sciences. The TN concentrations and $\delta^{15}N_{bulk}$ were analyzed on the freeze-dried, homogenized, and nonacidified bulk sediment samples. While for TOC concentrations and $\delta^{13}C_{org}$, samples were treated with 2 N HCl for 24 h to remove carbonates. In order to guarantee the complete removal of carbonates, the samples were treated with additional 2 N HCl for another 24 h. The decarbonated samples were recovered by centrifugation and then rinsed with deionized water, freeze-dried, homogenized, and weighed. The TOC and TN concentrations were determined using an Elementar Vario MACRO cube elemental analyzer. The analytical precision (RSD) is better than 0.5%. The $\delta^{13}C_{org}$ and $\delta^{15}N_{bulk}$ were measured on a Thermo MAT 253 mass spectrometer coupled to a Thermo elemental analyzer (FLASH 2000). The $\delta^{13}C_{org}$ and $\delta^{15}N_{bulk}$ values are represented in ‰ relative to the Vienna Peedee Belemnite (V-PDB) and to atmospheric N_2 standard, respectively. The uncertainties in the $\delta^{13}C_{org}$ and $\delta^{15}N_{bulk}$ values are within ±0.2‰ and ±0.4‰, respectively. We calculated the TOC mass accumulation rate (TOC-MAR) according to the equation: TOC-MAR = TOC×DBD×LSR, where DBD and LSR represent the bulk dry density (in units of mg/cm^3) and the linear sedimentation rate (in units of cm/kyr), respectively. The DBD data were from shipboard measurement (Tada et al., 2015). In addition, TOC concentration might be influenced by dilution effects from opal or detrital component, and thus it is generally normalized with a lithogenic element (e.g., Al or Ti) prior to paleoproductivity reconstruction (Tribovillard et al., 2006). In this study, Ti was employed to normalize TOC (i.e., TOC/Ti) in order to better evaluate organic carbon accumulation. Importantly, compared with the Ba_{EF} and biogenic silica flux, which can largely reflect primary production in ancient marine settings, the TOC flux recorded in sediments can vary substantially, since it is more susceptible to water redox conditions and postdepositional diagenesis (Schoepfer et al., 2015).

4. Results

4.1. Site U1425

The TOC and TN concentrations range from 0.4% to 4.9% (average 1.6%) and from 0.08% to 0.5% (average 0.2%), respectively (Figures 2d and 2e). The TOC and TN concentrations are high (average 2.8% and 0.3%, respectively) during 9.5–7.4 Ma, but uniformly low (average 1.2% and 0.2%, respectively) after 7.4 Ma. Similarly, the TOC-MAR values are much higher (30.2–145.2 mg/cm^2/kyr, average 84.5 mg/cm^2/kyr) during 9.5–7.4 Ma than those after 7.4 Ma (5.7–205.9 mg/cm^2/kyr, average 26.7 mg/cm^2/kyr) (Figure 3d). The C/N atomic ratios (hereafter referred to as C/N) vary from 3.6 to 13.8 (average 8.4), and also show a similar trend to that of TOC and TN concentrations, decreasing from an average of 10.8 during 9.5–7.4 Ma to an average of 7.5 after ~7.4 Ma (Figure 2f).

From 9.5 to 4 Ma, the $\delta^{13}C_{org}$ varies from −23.6 to −20.3‰ (average −21.8‰) and displays a weak increasing trend, followed by an overall decreasing trend after 4 Ma, with two less negative $\delta^{13}C_{org}$ excursions at ~3.6–3.1 Ma and ~1.5 Ma and a significant negative $\delta^{13}C_{org}$ excursion at ~0.5 Ma (Figure 2c). The $\delta^{15}N_{bulk}$ values range from 2.1 to 8.8‰ (average 4.3‰; Figure 2b). The $\delta^{15}N_{bulk}$ oscillates between 2.1 and 4.7‰ from 9.5 to 7.4 Ma and exhibits a long-term steady increasing trend to reach 5.6‰ from 7.4 to ~3.5 Ma, followed by a significant decreasing excursion (clustering around 4‰) at ~3.2–2.3 Ma. Later, it increases markedly to a maximum of 8.8‰ at ~1 Ma and then exhibits a decrease with a minimum of 3.1‰ at ~0.7 Ma. The rapid fluctuations of $\delta^{15}N_{bulk}$ and $\delta^{13}C_{org}$ since ~1.5 Ma were probably linked to periodical sea level changes and flux of the TWC.

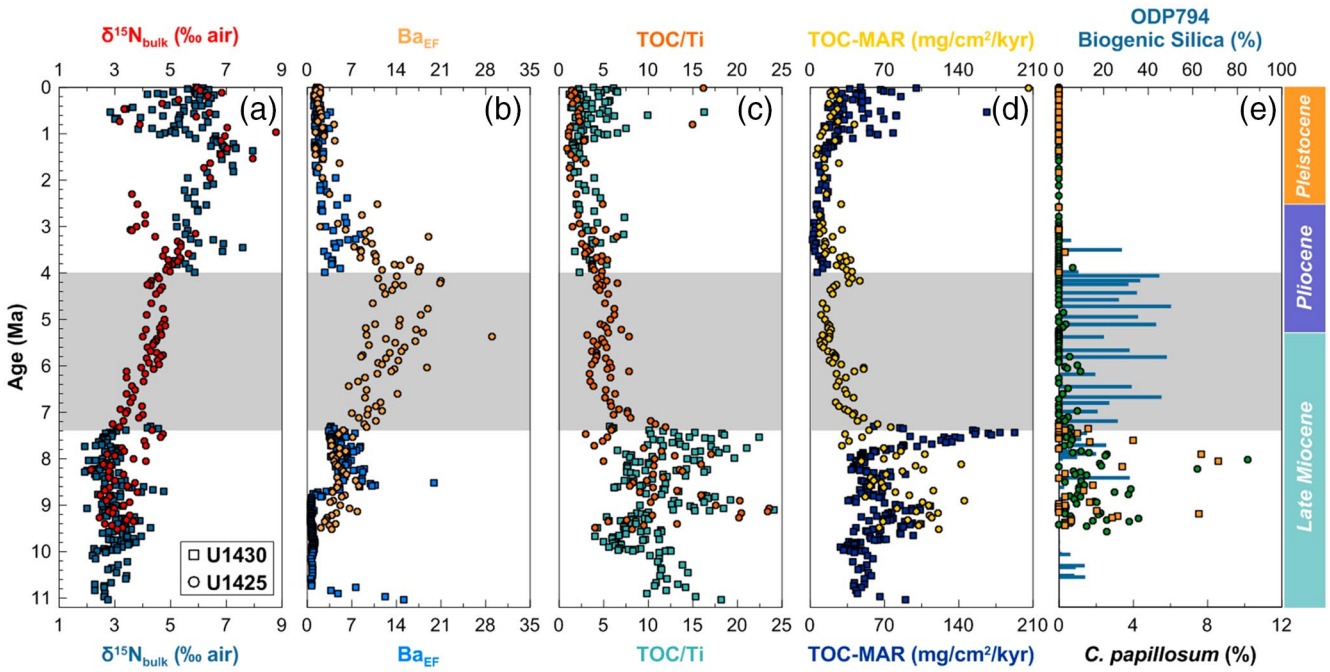

Figure 3. Variations of (a) $\delta^{15}N_{bulk}$, (b) Ba_{EF}, (c) TOC/Ti, (d) TOC-MAR (mg/cm^2/kyr), and (e) abundance of *C. papillosum* (Matsuzaki et al., 2018) at IODP Sites U1425 and U1430 since 11 Ma, along with biogenic silica content at ODP Site 794 since 11 Ma (Tada, 1994). IODP, Integrated Ocean Drilling Program; ODP, Ocean Drilling Program; TOC, total organic carbon; TOC-MAR, TOC mass accumulation rate.

The Ba concentrations range from 738 to 2,915 ppm from 9.5 to 7.4 Ma, followed by a significant increase during 7.4–4 Ma, culminating in a maximum of 8,517 ppm at ~4.2 Ma. The Ba concentrations then decline since 4 Ma (Figure 2g). The Al, K and Ti concentrations oscillate from 9.5 to 4 Ma, ranging from 2.6% to 8.3%, from 0.8% to 2.0%, and from 0.13% to 0.36%, respectively, and exhibit an overall increasing trend since 4 Ma with a negative shift at ~3.2 Ma (Figures 2h–2j).

4.2. Site U1430

From 11 to ~10 Ma, the TOC and TN concentrations and C/N are basically high, ranging from 2.5% to 4.1% (average 3.4%), from 0.28% to 0.38% (average 0.32%) and from 10.3 to 14.4 (average 12.4), respectively (Figures 2d–2F). However, the TOC-MAR values are relatively low because of the low LSR during this interval (Figure 3d). Generally, the TOC and TN concentrations and C/N at Site U1430 show similar values and temporal variations to those at Site U1425 from 9.5 to 7.4 Ma (Figure 2). Notably, the TOC-MAR values are extremely high because of the significantly increased LSR at ~7.6–7.4 Ma (Figure 2a). The TOC and TN concentrations, C/N and TOC-MAR all remain low after ~4 Ma before obvious rebounds at ~1.2 Ma (Figures 2 and 3).

The $\delta^{13}C_{org}$ at Site U1430 shows a slight increasing trend from 11 to 7.4 Ma and exhibits very similar values and temporal variations to those at Site U1425 after 9.5 Ma (Figure 2c). The $\delta^{15}N_{bulk}$ at Site U1430 also exhibits similar long-term trends to that observed at Site U1425 (Figure 2b). The only difference is that a significant $\delta^{15}N_{bulk}$ gradient (~2‰) exists between the two sites between ~4 and 2 Ma.

From 10.8 to 8.8 Ma, the Ba concentrations are abnormally low, followed by dramatic increases at ~8.8–8.5 Ma (Figure 2g), indicating preferential barium loss during early diagenesis in very reducing sediments (Schenau et al., 2001) and subsequent scavenging of barium from Ba-rich pore water at the sulfate-methane transition zone (Torres et al., 1996). The Ba concentrations at Site U1430 show similar values to those at Site U1425 from 8.5 to 7.4 Ma, and values remain relatively low after 4 Ma. The Al, K and Ti concentrations at Site U1430 basically exhibit similar variations to those at Site U1425 (Figures 2h–2j).

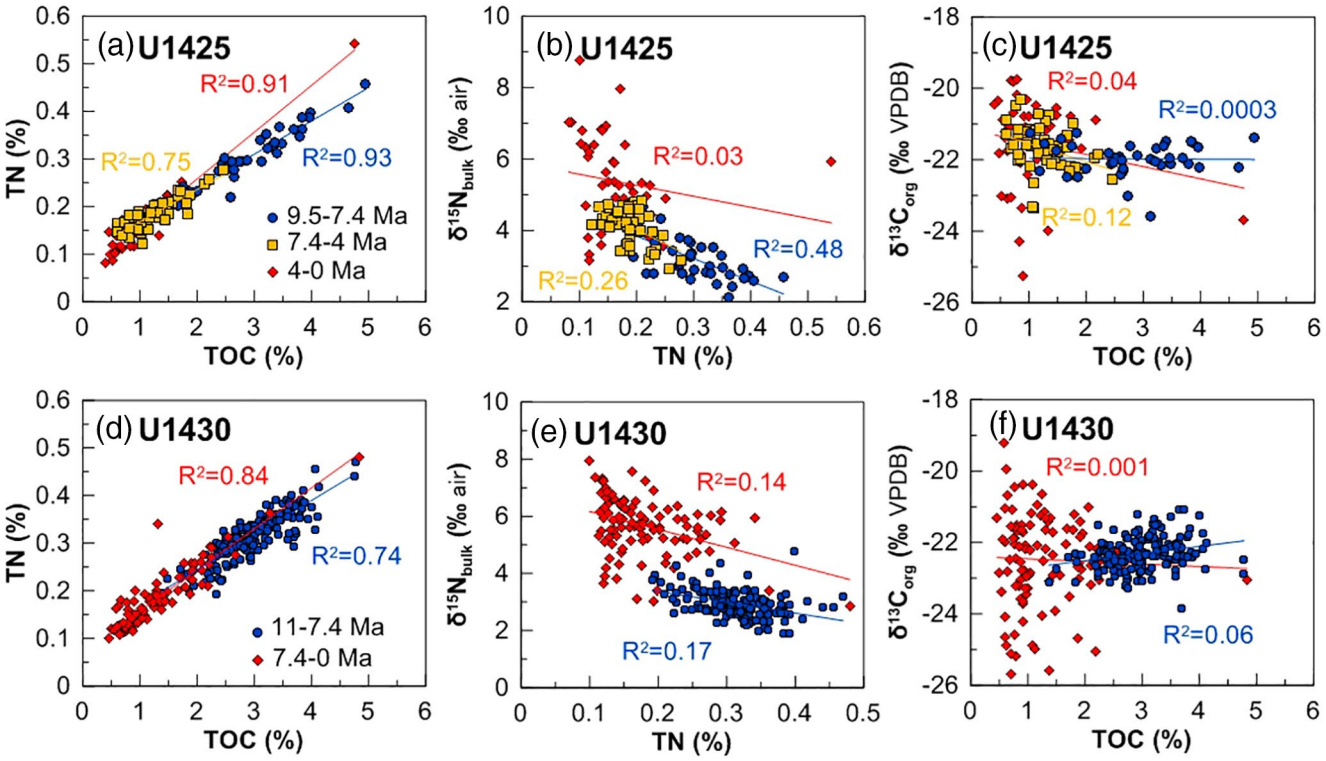

Figure 4. Geochemical cross-plots of TOC versus TN, TN versus $\delta^{15}N_{bulk}$, and TOC versus $\delta^{13}C_{org}$ from sediments at Sites U1425 (a–c) and U1430 (d–f). TN, total nitrogen; TOC, total organic carbon.

5. Discussions

5.1. Evaluation of Organic Carbon and Bulk Nitrogen Isotopes

The primary organic carbon and bulk nitrogen isotopic compositions can be modified by early and late burial diagenesis or allochthonous sources of nitrogen (Robinson et al., 2012). It is thus necessary to examine whether primary signatures preserved in sediments have been changed by postdepositional alteration.

Contribution from terrestrial runoff to the sedimentary organic matter reservoir should be minor due to a lack of large river input in the Japan Sea (Wang, 1999), and the $\delta^{13}C_{org}$ and C/N values further verified the principal marine origin of organic matters (Meyers, 1994; Figure S1). Plots of TOC versus TN for the two sites display strong linear correlation and an intercept on the TN axis (Figures 4a and 4d), which indicate the admixture of an organic component with a relatively constant $C_{organic}/N_{organic}$ ratio and an inorganic N component (Calvert, 2004). The intercepts on the TN axis (Figures 4a and 4d) reflect the occurrence of inorganic clay-bound nitrogen, which was mostly likely derived from terrigenous input, since the Japan Sea is a major sink of Asian dust (Irino & Tada, 2002; Nagashima et al., 2007; Shen et al., 2017). Such $\delta^{15}N$ signal commonly has relatively low values inherited from lands, which are close to the atmospheric $\delta^{15}N$ value (~0‰) with minor fractionation by land plants (Schubert & Calvert, 2001). Therefore, $\delta^{15}N_{inorg}$ contribution could not have led to a long-term positive offset in the $\delta^{15}N_{bulk}$ records from 7.4 to ~3.5 Ma (from ~3 to ~5.6‰ at Site U1425 and from ~3 to ~7.6‰ at Site U1430, respectively).

The $\delta^{15}N$ of sedimentary organic matter would increase during postdepositional alteration, as a consequence of preferential ^{14}N-remineralization (Möbius, 2013; Robinson et al., 2012). However, there is no obvious correlation between $\delta^{15}N_{bulk}$ and TN (Figures 4b and 4e). Also, the cross plot of $\delta^{13}C_{org}$ versus TOC does not show significant correlation (Figures 4c and 4f). The absence of covariance between these parameters indicates that original signatures of $\delta^{13}C_{org}$ and $\delta^{15}N_{bulk}$ are not likely to have been significantly altered by postdepositional processes at the two sites in the Japan Sea.

5.2. Evolution of Paleoproductivity and Deep-Water Redox Conditions

The biogeochemical nitrogen cycle is predominantly controlled by biological processes that are coupled to oxygen and carbon cycles (Fennel et al., 2005), and thus the nitrogen isotope signals preserved in marine sediments have the potential to reflect ocean redox conditions as well as metabolic processes and pathways (Robinson et al., 2012; Stüeken et al., 2016). On geological time scales, the sedimentary $\delta^{15}N_{bulk}$ should reflect the isotopic balance between different nitrogen sources, i.e. biological nitrogen fixation and upwelled bioavailable nitrogen (NO_3^- and NH_4^+) reaching the photic zone, to local biomass (Ader et al., 2016; Altabet et al., 2002; Falkowski, 1997; Quan et al., 2013; Sigman et al., 2009).

In this study, between 11 and ~7.4 Ma, $\delta^{15}N_{bulk}$ is characterized by low values in the profile ranging from 1.9 to 4.7‰ with an average of ~3‰ (Figure 3a). These values are isotopically higher than the nitrogen originated from N_2-fixation, but lower than those with significant denitrification (Tesdal et al., 2013). Above this horizon, $\delta^{15}N_{bulk}$ gradually increased to ~5‰ at site U1425 and ~6‰ at site U1430 between ~7.4 and 4 Ma.

Unlike the modern semi-closed Japan Sea, a deep-water connection existed with the North Pacific via northern deep seaways (>1,000 m) during the late Miocene-early Pliocene (S. Kamikuri and Motoyama, 2007; Matsuzaki et al., 2018; Tada, 1994). It has been reported that the North Pacific (20–40°N) at 1,000–3,000 m water depth was dominated by water of low dissolved oxygen content during the middle-late Miocene, the so-called oxygen minimum zone (OMZ), although with possible controversy for its existence (Tada, 1994; Woodruff & Savin, 1989); this OMZ structure could have exerted a major control on the formation of oxygen-deficient deep-water in the Japan Sea during this interval (Tada, 1994). The sulfur isotope of pyrite and redox-sensitive elements (e.g., Mn and U) at the Ocean Drilling Program (ODP) leg 127/128 sites indicated that deep-water fluctuated between suboxic to euxinic during 9–6.5 Ma in the Japan Sea (Masuzawa et al., 1992), approximately spanning the ~11–7.4 Ma interval with the latest reestablished age model (Kurokawa et al., 2019; Matsuzaki et al., 2018; Tada et al., 2015). Likewise, the coeval occasional occurrence of parallel laminations at sites U1425 and U1430 suggests the suppression of bioturbation due to low oxygen levels (Tada et al., 2015). Additionally, recent findings on the dominant occurrence of *C. papillosum* between 9.5 and 7.4 Ma at Sites U1425 and U1430, which inhabits oxygen-poor waters at depths of 1,000–3,000 m in the North Pacific, also suggested oxygen-deficient deep-water in the Japan Sea (Matsuzaki et al., 2018, Figure 3e). Moderate Ba_{EF} combined with high TOC/Ti and TOC-MAR (Figures 3b–3d) at sites U1425 and U1430, indicative of moderate biological productivity but high organic matter burial, further supported the scenario of oxygen-poor bottom water in the Japan Sea during the ~11–7.4 Ma interval.

Low $\delta^{15}N_{bulk}$ values, similar to the range reported by our study, are commonly observed in ancient anoxic systems, such as the black shales of the mid-Cretaceous and the Oceanic Anoxic Event (OAE), as well as in the more recently deposited sediments in the Black Sea and the Cariaco Basin, which are regarded to have been mainly caused by N_2-fixation or assimilation of ammonia with a large isotopic fractionation effect under anoxic water column conditions (e.g., Coban-Yıldız et al., 2006; Higgins et al., 2012; Junium & Arthur, 2007; Thunell et al., 2004). $\delta^{15}N_{bulk}$ values ranging between −2 and 1‰ are most likely linked to biological N_2-fixation with Mo-based nitrogenase in surface waters compensating for significant loss of nitrogen via denitrification/anammox (Fulton et al., 2012; Haug et al., 1998; Quan et al., 2013), while the more likely explanation for anomalously low $\delta^{15}N_{bulk}$ values (<−2‰) in sediments is biological N_2-fixation with V- or Fe-based nitrogenases (X. Zhang et al., 2014) or partial assimilation of upwelled NH_4^+ (Higgins et al., 2012). The deep-water in the Japan Sea has been proved to be intermittently anoxic when the organic-rich sediments formed during 11 to 7.4 Ma, as discussed above, with relatively lower $\delta^{15}N_{bulk}$ values compared to those of other time intervals. We propose that oxygen-deficient deep-water may have facilitated (nearly) complete denitrification, thus resulting in lower $\delta^{15}N_{bulk}$ values in sediments (Quan et al., 2013). Alternatively, in the redox-stratified Japan Sea, denitrification may have led to bioavailable nitrogen (i.e., nitrate) deficits in the photic zone due to severe loss of fixed nitrogen, which possibly stimulated N_2-fixation with Mo-based nitrogenase as an important contributor to the ecosystem, imprinting low $\delta^{15}N$ values on sediments (Fulton et al., 2012; Haug et al., 1998; Sigman et al., 2009). These two processes, however, are not mutually exclusive between each other. With progressive denitrification, N derived from N_2-fixation can be main N source. Given that the redox transition zone in the Japan Sea during that interval is poorly constrained, it is difficult to confirm proportion of N from different sources.

From ~7.4 to 4 Ma, the productivity proxy Ba_{EF} exhibited sustained increases (Figure 3b), indicating enhanced biological production, which is further supported by the greatly elevated biogenic silica contents at ODP Site 794 in the Japan Sea (Tada, 1994; Figure 3e). These data imply that the surface waters had high concentrations of nutrients and fueled high production of biogenic silica during this interval. The enhanced biological production recorded in the Japan Sea is basically coincident with "biogenic bloom" widely observed in eutrophic regions, and most pronounced in upwelling systems of the Indian and Pacific oceans (Dickens & Owen, 1999; Farrell et al., 1995; Y. Zhang et al., 2017), and even in some low-nutrient or oligotrophic regions (Hermoyian & Owen, 2001) during the late Miocene to early Pliocene. The timing of higher primary production varies significantly among regions, which may reflect changes in global nutrient cycling imposed by regional factors (Lyle et al., 2019). Such worldwide increased bioproduction is thought to have resulted from globally increased nutrient supply to the oceans, which is likely associated with intensification of the Asian monsoon and uplift of the Himalayas-Tibetan Plateau during the late Miocene (Cermeño et al., 2015; Diester-Haass et al., 2006) and/or redistribution of nutrients within the oceans (Dickens & Owen, 1999).

In contrast to the substantial rise in biological production during 7.4–4 Ma, the coeval organic burial sharply declined as shown by decreased TOC/Ti and TOC-MAR values (Figure 3). The preservation of organic matter is largely controlled by exposure time to oxygen in water (Hartnett et al., 1998), and thus low sedimentation rates and/or elevated water oxygen concentrations will potentially lead to poor organic burial (Tyson, 2005). Given the constant sedimentation rates before and after 7.4 Ma at Site U1425, decreases in organic burial were thus interpreted as the result of elevated bottom-water oxygen. Muted enrichment of redox-sensitive trace elements along with intense bioturbation also supports the presence of oxic deep-water (Kurokawa et al., 2019; Masuzawa et al., 1992; Tada, 1994; Tada et al., 2015). However, the corresponding $\delta^{15}N_{bulk}$ values can reach ~5‰–6‰ during this interval. Thematically, high $\delta^{15}N_{bulk}$ value can be used to reflect incomplete denitrification under anoxic conditions, which also means that the anoxic waters did not prevail. For the Japan Sea, elevated surface productivity may have resulted in prominent organic respiration within the water column. Such a situation could lower the oxygen content in mid-depth water masses and increase the $\delta^{15}N$ of residual nitrate pool. The mid-depth low oxygen condition could be also facilitated by the intensified East Asian winter monsoon at that time (Matsuzaki et al., 2020). These isotopically heavy $\delta^{15}N$ could be fingerprinted by sediments underlying this low-oxygen zone. It is also possible that upwelling supplied more nutrients to the surface water and resulted in higher primary production. Therefore, the correspondence of high-biological production and low-organic preservation highlight the role of enhanced deep-water ventilation in breaking vertical stratification and promoting biological production in the Japan Sea during the late Miocene-early Pliocene.

5.3. Potential Influences of Tectonic- and Eustatic-Driven Changes and Southern Ocean Ventilation Changes

Tectonic- and eustatic-driven changes played a significant role in regulating the sill depths of the seaways connecting the Japan Sea and the Pacific Ocean, and also influenced the properties (oxic/anoxic) of water flowing into the Japan Sea (Tada, 1994). After ~10.5 Ma, the Japan Sea was connected to the North Pacific via eastern (around the present Honshu area) and northern (between the northern Honshu and southern Hokkaido islands) seaways (Figures 1c–1f), and the northern seaway was deep enough (>1,000 m) to allow deep water from the North Pacific to enter the Japan Sea (S. Kamikuri and Motoyama, 2007). The uplift of the Ou Backbone Range at 12—9 Ma (Figure 5a) gradually shoaled and closed the eastern seaway (Nakajima et al., 2006), while the northern seaway remained unchanged prior to ~4.5 Ma as demonstrated by seawater neodymium isotopic composition records which indicate that deep-water exchange between the North Pacific and the Japan Sea rapidly ceased at 4.5 Ma due to the shoaling/narrowing of northern seaway driven by active tectonic uplift in the northern Japan arc at that time (Kozaka et al., 2018; Figure 5a). This is further supported by largely constant sedimentation rates in the Pacific off northern Japan from 10 to ~5 Ma (Motoyama et al., 2004) and an initial rise of sedimentary basins in southwestern Hokkaido at ~4.5 Ma (Sagayama, 2002). Given the absence of obvious uplift around the northern Japan arc at ~7.4 Ma, oxygenation of the Japan Sea was unlikely to be caused by regional tectonic evolution. In addition, the global sea-level

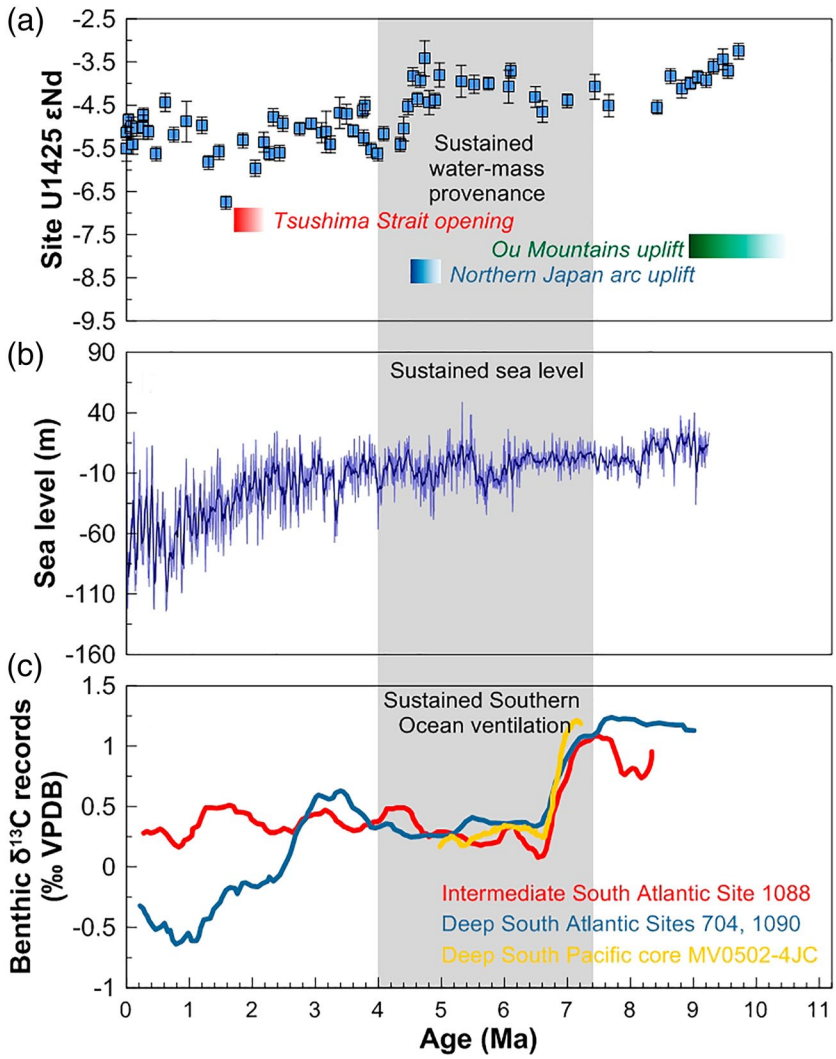

Figure 5. Potential drivers for deep-water oxygenation of the Japan Sea, including (a) regional tectonic activities around the Japan Sea (Kozaka et al., 2018; Nakajima et al., 2006), (b) global sea level, based on oxygen isotope records (Miller et al., 2005), and (c) Southern Ocean ventilation, based on benthic $\delta^{13}C$ records from subAntarctic Atlantic Sites 1088, 704 and 1092 (Hodell & Venz-Curtis, 2006) and subAntarctic Pacific core MV0502-4JC (Waddell et al., 2009). The gray shading highlights enhanced biological productivity and deep-water ventilation in the Japan Sea during ~7.4–4 Ma.

remained relatively stable at ~7.4 Ma (Miller et al., 2005; Figure 5b), precluding the sea-level changes as a causal factor for oxygenation of the Japan Sea.

The deep waters in the western North Pacific involve Lower Circumpolar Deep Water (LCDW), an advective flow from the Southern Ocean, and North Pacific Deep Water (NPDW) originated from vertical mixing of LCDW with subsurface water masses of the North Pacific (Kawabe & Fujio, 2010; Whitworth III et al., 1999; Figure 1a). The modern Southern Ocean plays a key role in ventilating the world's major oceans through the energetic deep-reaching Antarctic Circumpolar Current (Marshall & Speer, 2012). Therefore, changes in deep-water circulation in the Southern Ocean, if they occurred, may have affected redox conditions of the water mass flowing into the Japan Sea during the late Miocene-early Pliocene. A comparison of benthic foraminiferal $\delta^{13}C$ profiles between intermediate water (2,082 m) at ODP Site 1088 and deep water (2,532/3,702 m) at ODP Sites 704/1090 in the subAntarctic Atlantic exhibits no vertical $\delta^{13}C$ gradient and provides evidence for constant vertical mixing in the South Ocean during ~7.4–4 Ma (Hodell & Venz-Curtis, 2006; Figure 5c). Likewise, the almost identical changes of $\delta^{13}C$ records from the deep subAntarctic

Pacific core MV0502-4JC (4,286 m) with those from Sites 704/1092 during the end Miocene indicate that the deep waters between the Atlantic and Pacific sectors of the Southern Ocean remained homogenous at that time (Waddell et al., 2009; Figure 5c). The lack of any vertical or interbasinal isotope gradients within the Southern Ocean indicates that deep-water ventilation in the Southern Ocean was largely stable across ~7.4 Ma. Therefore, deep-water circulation in the Southern Ocean could not act as a driver for deep-water oxygenation in the Japan Sea during the late Miocene-early Pliocene.

5.4. Deep-Ocean Oxygenation in the Japan Sea Caused by Deep-Water Formation in the North Pacific

We suggest, therefore, that deep-water formation in the North Pacific is the more likely mechanism responsible for the deep-water oxygenation and elevated biological production in the Japan Sea at ~7.4 Ma. It is unlikely to be ascribed to intermediate-water formation in the North Pacific, mainly because the radiolaria in the Japan Sea dominantly related to subarctic intermediate cold waters of the North Pacific, such as *Pseudodictyophimus gracilipes* (Bailey), *Spongopyle osculosa* Dreyer, and *Cycladophora davisiana*, did not increase significantly during the late Miocene (Matsuzaki et al., 2018). And notably, *C. davisiana*, now most abundantly in well-oxygenated intermediate-waters of the Sea of Okhotsk (Nimmergut & Abelmann, 2002), have widely existed in the western Bering during the last glacial period, indicative of the formation of cold, well-oxygenated intermediate-water similar to the modern Okhotsk intermediate water (Ohkushi et al., 2003); whereas this species increased substantially in the Japan Sea after ~3.2 Ma, in response to the expansion of the Northern Hemisphere Glaciation (Matsuzaki et al., 2018). Such radiolarian assemblage changes probably indicate that intermediate-water ventilation closely related to sea ice expansion may not have increased in the western North Pacific in the late Miocene. Importantly, the occurrence of radiolarian species in the Japan Sea, which were related to the North Pacific deep-water, highlight the presence of deep water masses derived from the North Pacific during the late Miocene-early Pliocene (S. Kamikuri and Motoyama, 2007). In the scenario of deep-water formation, the chemocline above oxygen-deficient deep-water in the North Pacific would have deteriorated, allowing the inflow of oxygenated water into the Japan Sea. The contemporary intensified East Asian winter monsoon (Matsuzaki et al., 2020) was favorable for active lateral and vertical water circulation, and thus the oxygenated deep-water from the North Pacific could permeate into different depths. Moreover, enhanced upwelling could provide abundant nutrients for photosynthetic organisms in surface water and led to sharp, marked increases in biological productivity. Deep-water ventilation in turn resulted in poor organic matter preservation in the Japan Sea (Figure 6c). Additionally, the sedimentary records may also support deep-water formation in the North Pacific during the late Miocene-early Pliocene. Sediment hiatuses were recognized in slope regions not only in the Japan Sea (~7.3 Ma; Site U1430) (Matsuzaki et al., 2018; Tada et al., 2015) but also outside the Japan Sea in the North Pacific (~7 Ma; Site 1150, 2,681 m and Site 1151, 2,178 m) (Motoyama et al., 2004). The synchronous onset of these hiatuses probably resulted from winnowing and sweeping by erosive ocean bottom currents during deep-water formation in the North Pacific.

Previous studies suggested that North Pacific deep-water could form during the last deglacial abrupt cold events due to increased surface salinity driven by subdued local freshwater flux (Okazaki et al., 2010; Rae et al., 2014, 2020; Yu et al., 2020). Precipitation in the North Pacific mid-latitudes is mainly shaped by the storm tracks, the position of which can be affected by the equator-to-pole temperature gradient (Brayshaw et al., 2008; Shaw et al., 2016). A sustained global cooling occurred in the late Miocene as demonstrated by SST reconstructions in global oceans (Herbert et al., 2016; Figure 6a). High-latitude amplification of cooling in the North Hemisphere led to the intensified meridional SST gradients, which probably could push the storm tracks southward and lead to decreased precipitation in mid-latitude North Pacific. A weakened East Asian summer monsoon during this period (Steinke et al., 2010; Wan et al., 2010; Figure 6b) probably conveyed less moisture to the North Pacific (Emile-Geay et al., 2003), and thus could also result in decreased rainfall in this region. In this context, declines in precipitation in mid-latitude regions could have induced substantial increases in surface salinity of the North Pacific. More saline and oxygen-rich surface water would act directly to erode the halocline and facilitate deep-water formation. Higher salinity in the North Pacific may also be driven by increased delivery of more saline subtropical waters into the North Pacific due to an intensification of the westerly winds in the presence of pronounced cooling in the North Hemisphere

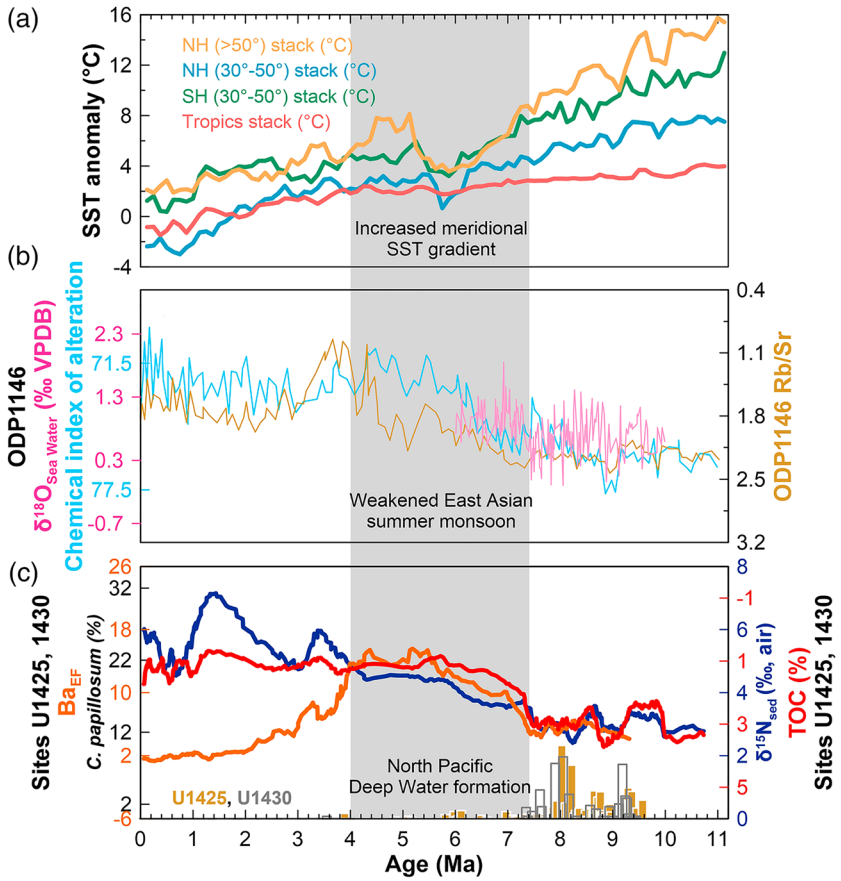

Figure 6. Proxy records of nutrient utilization and paleoproductivity in the Japan Sea are compared to regional and global paleoclimate and paleoceanographic reconstructions since 11 Ma. (a) Global SST anomalies (Herbert et al., 2016). (b) Chemical index of alteration (CIA) and Rb/Sr at ODP Sites 1146 (Wan et al., 2010) and local $\delta^{18}O$ seawater estimates at ODP Site 1146 (Steinke et al., 2010). (c) Nutrient utilization and productivity records at Sites U1425 and U1430 including $\delta^{15}N_{bulk}$, Ba_{EF} and TOC shown by 11-pt running mean, along with abundance of *C. papillosum* inhabiting oxygen-depleted deep water in the Japan Sea (Matsuzaki et al., 2018). The gray shading highlights enhanced biological productivity and deep-water ventilation in the Japan Sea during ~7.4–4 Ma. ODP, Ocean Drilling Program; SST, sea surface temperature; TOC, total organic carbon.

(Gray et al., 2018; Rae et al., 2020). The late Miocene global cooling may also have caused enhanced Ekman suction in the North Pacific, which could bring up salt from subsurface waters and lead to increased salinity in surface layer (Gray et al., 2018; Okazaki et al., 2010). Besides, changes in the pycnocline depth and dissolved oxygen content of surface seawater due to the cooling probably could also play a role in deep ocean ventilation. More proxy records and simulation works are needed to test the mechanisms mentioned above in the future.

6. Conclusions

The $\delta^{13}C_{org}$ and $\delta^{15}N_{bulk}$ records and paleoproductivity proxy Ba_{EF} in sediments from IODP Sites U1425 and U1430 were used to constrain paleoproductivity and redox conditions in the Japan Sea, and also to monitor deep-water circulation in the North Pacific. The deep-water was intermittently anoxic in the Japan Sea before ~7.4 Ma, with moderate Ba_{EF} but remarkably high TOC flux. The low $\delta^{15}N_{bulk}$ values in these organic-rich sediments likely reflect nearly complete denitrification. During ~7.4–4 Ma gradually increased Ba_{EF} values indicate increased biological production. However, the coeval TOC, TOC/Ti, and TOC-MAR sharply decreased, implying intense degradation of organic matter prior to burial. Such poor organic preservation was mainly driven by the oxygenation in the Japan Sea during this interval. We propose that deep-water

formation in the North Pacific played a crucial role in deep-water ventilation in the Japan Sea via northern deep seaways. Increased equator-to-pole SST gradients in response to the late Miocene global cooling may have decreased precipitation in mid-latitude regions through southward shift of mid-latitude storm tracks, in combination with the weakened East Asian summer monsoon and the resultant decreased moisture transport, generating more saline surface water and further leading to deep-water formation in the North Pacific.

Data Availability Statement

All data necessary to assess the validity of this research are archived at NOAA's National Centers for Environmental Information (https://www.ncdc.noaa.gov/paleo/study/30892).

Acknowledgments
The authors acknowledge the Integrated Ocean Drilling Program and the scientific party and technicians of IODP Expedition 346 for recovering the samples. We also thank Matthew Huber, Becky Robinson, Phil Meyers and two anonymous reviewers for their constructive comments to improve this manuscript. This work was supported by the National Natural Science Foundation of China (41806058), Strategic Priority Research Program of the Chinese Academy of Sciences (XDB40010100), National Natural Science Foundation of China (42076052, 41622603, 41576034, U1606401), Open Fund of the Key Laboratory of Marine Geology and Environment, CAS (MGE2019KG15), Innovation Project (2016ASKJ13, MGQNLM-TD201805, MGQNLM-KF202001), Taishan and Aoshan Talents Program (2017ASTCP-ES01) and China Postdoctoral Science Foundation (2018M632729).

References

Ader, M., Thomazo, C., Sansjofre, P., Busigny, V., Papineau, D., Laffont, R., et al. (2016). Interpretation of the nitrogen isotopic composition of Precambrian sedimentary rocks: Assumptions and perspectives. *Chemical Geology*, *285*, 35537–35550. http://dx.doi.org/10.1016/j.chemgeo.2016.02.010

Altabet, M. A., Higginson, M. J., & Murray, D. W. (2002). The effect of millennial-scale changes in Arabian Sea denitrification on atmospheric CO_2. *Nature*, *415*, 159–162. https://doi.org/10.1038/415159a

Brayshaw, D. J., Hoskins, B. J., & Blackburn, M. (2008). The storm-track response to idealized SST perturbations in an aquaplanet GCM. *Journal of the Atmospheric Sciences*, *65*(9), 2842–2860. https://doi.org/10.1175/2008JAS2657.1

Burls, N. J., Fedorov, A. V., Sigman, D. M., Jaccard, S. L., Tiedemann, R., & Haug, G. H. (2017). Active Pacific meridional overturning circulation (PMOC) during the warm Pliocene. *Science Advances*, *3*, e1700156. https://doi.org/10.1126/sciadv.1700156

Calvert, S. E. (2004). Beware intercepts: Interpreting compositional ratios in multi-component sediments and sedimentary rocks. *Organic Geochemistry*, *35*(8), 981–987. https://doi.org/10.1016/j.orggeochem.2004.03.001

Cerling, T. E., Harris, J. M., MacFadden, B. J., Leakey, M. G., Quade, J., Eisenmann, V., et al. (1997). Global vegetation change through the Miocene/Pliocene boundary. *Nature*, *389*(6647), 153–158. https://doi.org/10.1038/38229

Cermeño, P., Falkowski, P. G., Romero, O. E., Schaller, M. F., & Vallina, S. M. (2015). Continental erosion and the cenozoic rise of marine diatoms. *Proceedings of the National Academy of Sciences of the United States of America*, *112*(14), 4239–4244. https://doi.org/10.1073/pnas.1412883112

Coban-Yıldız, Y., Altabet, M. A., Yılmaz, A., & Tuğrul, S. (2006). Carbon and nitrogen isotopic ratios of suspended particulate organic matter (SPOM) in the Black Sea water column. *Deep-Sea Research Part II*, *53*(17), 1875–1892. https://doi.org/10.1016/j.dsr2.2006.03.021

Dickens, G. R., & Owen, R. M. (1999). The latest Miocene–early Pliocene biogenic bloom: A revised Indian Ocean perspective. *Marine Geology*, *161*(1), 75–91. https://doi.org/10.1016/S0025-3227(99)00057-2

Diester-Haass, L., Billups, K., & Emeis, K. C. (2006). Late Miocene carbon isotope records and marine biological productivity: Was there a (dusty) link? *Paleoceanography*, *21*(4), PA4216. https://doi.org/10.1029/2006PA001267

Emile-Geay, J., Cane, M. A., Naik, N., Seager, R., Clement, A. C., & van Geen, A. (2003). Warren revisited: Atmospheric freshwater fluxes and "Why is no deep water formed in the North Pacific". *Journal of Geophysical Research*, *108*(C6), 3178. https://doi.org/10.1029/2001JC001058

Falkowski, P. G. (1997). Evolution of the nitrogen cycle and its influence on the biological sequestration of CO_2 in the ocean. *Nature*, *387*, 272–275. https://doi.org/10.1038/387272a0

Farrell, J. W., Raffi, I., Janecek, T. R., Murray, D. W., Levitan, M., Dadey, K. A., et al. (1995). Late Neogene sedimentation patterns in the eastern equatorial Pacific Ocean. In N. Pisias, L. Mayer, T. Janecek, A. Palmer-Julson, & T. H. van Andel (Eds.), *Proceedings of the ocean drilling Program, scientific results*. Vol. 138 (pp. 717–756). College Station, TX: Ocean Drilling Program. https://doi.org/10.2973/odp.proc.sr.138.143.1995

Fennel, K., Follows, M., & Falkowski, P. G. (2005). The co-evolution of the nitrogen, carbon and oxygen cycles in the Proterozoic ocean. *American Journal of Science*, *305*(6–8), 526–545. https://doi.org/10.2475/ajs.305.6-8.526

Ferreira, D., Cessi, P., Coxall, H. K., de Boer, A., Dijkstra, H. A., Drijfhout, S. S., et al. (2018). Atlantic-Pacific asymmetry in deep water formation. *Annual Review of Earth and Planetary Sciences*, *46*, 327–352. https://doi.org/10.1146/annurev-earth-082517-010045

Fulton, J. M., Arthur, M. A., & Freeman, K. A. (2012). Black Sea nitrogen cycling and the preservation of phytoplankton $\delta^{15}N$ signals during the Holocene. *Global Biogeochemical Cycles*, *26*, GB2030. https://doi.org/10.1029/2011GB004196

Gallagher, S. J., Kitamura, A., Iryu, Y., Itaki, T., Koizumi, I., & Hoiles, P. W. (2015). The Pliocene to recent history of the Kuroshio and Tsushima currents: A multi-proxy approach. *Progress in Earth and Planetary Science*, *2*, 17. https://doi.org/10.1186/s40645-015-0045-6

Gamo, T., Nakayama, N., Takahata, N., Sano, Y., Zhang, J., Yamazaki, E., et al. (2014). The Sea of Japan and its unique chemistry revealed by time-series observations over the last 30 years. *Monographs on Environment, Earth and Planets*, *2*, 1–22. https://doi.org/10.5047/meep.2014.00201.0001

Gong, X., Lembke-Jene, L., Lohmann, G., Knorr, G., Tiedemann, R., Zou, J., et al. (2019). Enhanced North Pacific deep-ocean stratification by stronger intermediate water formation during Heinrich Stadial 1. *Nature Communications*, *10*, 656. https://doi.org/10.1038/s41467-019-08606-2

Gray, W. R., Rae, J. W. B., Wills, R. C. J., Shevenell, A. E., Taylor, B., Burke, A., et al. (2018). Deglacial upwelling, productivity and CO_2 outgassing in the North Pacific Ocean. *Nature Geoscience*, *11*, 340–344. https://doi.org/10.1038/s41561-018-0108-6

Gungor, A., Lee, G. H., Kim, H. G., Han, H. C., Kang, M. H., Kim, J., et al. (2012). Structural characteristics of the northern Okinawa Trough and adjacent areas from regional seismic reflection data: Geologic and tectonic implications. *Tectonophysics*, *522*(523), 198–207. https://doi.org/10.1016/j.tecto.2011.11.027

Hanagata, S. (2003). Miocene-Pliocene foraminifera from the Niigata oil-fields region, northeastern Japan. *Micropaleontology*, *49*(4), 293–340. https://doi.org/10.1661/0026-2803(2003)049[0293:MFFTNO]2.0.CO;2

Hartnett, H. E., Keil, R. G., Hedges, J. I., & Devol, A. H. (1998). Influence of oxygen exposure time on organic carbon preservation in continental marine regions. *Nature*, *391*, 572–575. https://doi.org/10.1038/35351

Haug, G. H., Pedersen, T. F., Sigman, D. M., Calvert, S. E., Nielsen, B., & Peterson, L. C. (1998). Glacial/interglacial variations in production and nitrogen fixation in the Cariaco Basin during the last 580 kyr. *Paleoceanography*, *13*(5), 427–432. https://doi.org/10.1029/98PA01976

Herbert, T. D., Lawrence, K. T., Tzanova, A., Peterson, L. C., Caballerogill, R., & Kelly, C. S. (2016). Late Miocene global cooling and the rise of modern ecosystems. *Nature Geoscience*, *9*, 843–847. https://doi.org/10.1038/ngeo2813

Hermoyian, C. S., & Owen, R. M. (2001). Late Miocene-early Pliocene biogenic bloom: Evidence from low-productivity regions of the Indian and Atlantic Oceans. *Paleoceanography*, *16*(1), 95–100. https://doi.org/10.1029/2000PA000501

Higgins, M. B., Robinson, R. S., Husson, J. M., Carter, S. J., & Pearson, A. (2012). Dominant eukaryotic export production during ocean anoxic events reflects the importance of recycled NH_4^+. *Proceedings of the National Academy of Sciences of the United States of America*, *109*(7), 2269–2274. https://doi.org/10.1073/pnas.1402976111

Hodell, D. A., & Venz-Curtis, K. A. (2006). Late Neogene history of deepwater ventilation in the Southern Ocean. *Geochemistry, Geophysics, Geosystems*, *7*, Q09001. https://doi.org/10.1029/2005GC001211

Holbourn, A. E., Kuhnt, W., Clemens, S. C., Kochhann, K. G. D., Jöhnck, J., Lübbers, J., et al. (2018). Late Miocene climate cooling and intensification of southeast Asian winter monsoon. *Nature Communications*, *9*, 1584. https://doi.org/10.1038/s41467-018-03950-1

Horozal, S., Kim, G. Y., Cukur, D., Bahk, J. J., & Kim, S. P. (2017). Sedimentary and structural evolution of the Eastern South Korea Plateau (ESKP), East Sea (Japan Sea). *Marine and Petroleum Geology*, *85*, 70–88. https://doi.org/10.1016/j.marpetgeo.2017.04.014

Iijima, A., & Tada, R. (1990). Evolution of Tertiary sedimentary basins of Japan in reference to opening of the Japan Sea. *Journal of the Faculty of Science*, *22*(2), 121–171.

Irino, T., & Tada, R. (2002). High-resolution reconstruction of variation in aeolian dust (Kosa) deposition at ODP site 797, the Japan Sea, during the last 200 ka. *Global and Planetary Change*, *35*, 143–156. https://doi.org/10.1016/S0921-8181(02)00135-2

Itaki, T. (2016). Transitional changes in microfossil assemblages in the Japan Sea from the late Pliocene to early Pleistocene related to global climatic and local tectonic events. *Progress in Earth and Planetary Science*, *3*, 11. https://doi.org/10.1186/s40645-016-0087-4

Jaccard, S. L., & Galbraith, E. D. (2013). Direct ventilation of the North Pacific did not reach the deep ocean during the last deglaciation. *Geophysical Research Letters*, *40*(1), 199–203. https://doi.org/10.1029/2012GL054118

Jenkyns, H. C. (2003). Evidence for rapid climate change in the Mesozoic–Palaeogene greenhouse world. *Philosophical Transactions of the Royal Society A*, *361*(1810), 1885–1916. https://doi.org/10.1098/rsta.2003.1240

Jenkyns, H. C. (2010). Geochemistry of oceanic anoxic events. *Geochemistry, Geophysics, Geosystems*, *11*(3), Q03004. https://doi.org/10.1029/2009GC002788

Jolivet, L., Tamaki, K., & Fournier, M. (1994). Japan Sea, opening history and mechanism: A synthesis. *Journal of Geophysical Research*, *99*, 22237–22259. https://doi.org/10.1029/93JB03463

Junium, C. K., & Arthur, M. A. (2007). Nitrogen cycling during the Cretaceous, Cenomanian-Turonian Oceanic Anoxic Event II. *Geochemistry, Geophysics, Geosystems*, *8*(3), Q03002. https://doi.org/10.1029/2006GC001328

Kamikuri, S., & Motoyama, I. (2007). Radiolarian assemblage and environmental changes in the Japan Sea since the late Miocene. *Fossils*, *82*, 35–42.

Kamikuri, S. I., Itaki, T., Motoyama, I., & Matsuzaki, K. M. (2017). Radiolarian biostratigraphy from middle Miocene to late Pleistocene in the Japan Sea. *Paleontological Research*, *21*(4), 397–421. https://doi.org/10.2517/2017PR001

Kawabe, M., & Fujio, S. (2010). Pacific ocean circulation based on observation. *Journal of Oceanography*, *66*(3), 389–403. https://doi.org/10.1007/s10872-010-0034-8

Kozaka, Y., Horikawa, K., Asahara, Y., Amakawa, H., & Okazaki, Y. (2018). Late Miocene–mid-Pliocene tectonically induced formation of the semi-closed Japan Sea, inferred from seawater Nd isotopes. *Geology*, *46*(10), 903–906. https://doi.org/10.1130/G45033.1

Kurokawa, S., Tada, R., Matsuzaki, K. M., Irino, T., & Johanna, L. (2019). Cyclostratigraphy of the late Miocene to Pliocene sediments at IODP sites U1425 and U1430 in the Japan Sea and paleoceanographic implications. *Progress in Earth and Planetary Science*, *6*, 2. https://doi.org/10.1186/s40645-018-0250-1

Lyle, M., Drury, A. J., Tian, J., Wilkens, R., & Westerhold, T. (2019). Late Miocene to Holocene high-resolution eastern equatorial Pacific carbonate records: Stratigraphy linked by dissolution and paleoproductivity. *Climate of the Past*, *15*, 1715–1739. https://doi.org/10.5194/cp-15-1715-2019

Marshall, J., & Speer, K. (2012). Closure of the meridional overturning circulation through Southern Ocean upwelling. *Nature Geoscience*, *5*(5), 171–180. https://doi.org/10.1038/ngeo1391

Masuzawa, T., Takada, J., & Matsushita, R. (1992). Trace-element geochemistry of sediments and sulfur isotope geochemistry of framboidal pyrite from Site 795, Leg 127, Japan Sea. In K. A. Pisciotto, J. C. IngleJr, & M. T. von Breymann (Eds.), *Proceedings of the ocean drilling program, scientific results*. 127/128 (pp. 705–717). https://doi.org/10.2973/odp.proc.sr.127128-1.179.1992

Matsuzaki, K. M., Itaki, T., Tada, R., & Kamikuri, S. (2018). Paleoceanographic history of the Japan Sea over the last 9.5 million years inferred from radiolarian assemblages (IODP Expedition 346 Sites U1425 and U1430). *Progress in Earth and Planetary Science*, *5*, 54. https://doi.org/10.1186/s40645-018-0204-7

Matsuzaki, K. M., Suzuki, N., & Tada, R. (2020). An intensifed East Asian winter monsoon in the Japan Sea between 7.9 and 6.6 Ma. *Geology*, *48*(9), 919–923. https://doi.org/10.1130/G47393.1

Max, L., Lembke-Jene, L., Riethdorf, J.-R., Tiedemann, R., Nürnberg, D., Kühn, H., et al. (2014). Pulses of enhanced North Pacific Intermediate Water ventilation from the Okhotsk Sea and Bering Sea during the last deglaciation. *Climate of the Past*, *10*, 591–605. https://doi.org/10.5194/cp-10-591-2014

Meyers, P. A. (1994). Preservation of elemental and isotopic source identification of sedimentary organic matter. *Chemical Geology*, *114*, 289–302. https://doi.org/10.1016/0009-2541(94)90059-0

Miller, K. G., Kominz, M. A., Browning, J. V., Wright, J. D., Mountain, G. S., Katz, M. E., et al. (2005). The Phanerozoic record of global sea-level change. *Science*, *310*(5752), 1293–1298. https://doi.org/10.1016/0009-2541(94)90059-0

Möbius, J. (2013). Isotope fractionation during nitrogen remineralization (ammonification): Implications for nitrogen isotope biogeochemistry. *Geochimica et Cosmochimica Acta*, *105*, 422–432. https://doi.org/10.1016/j.gca.2012.11.048

Motoyama, I., Niitsuma, N., Maruyama, T., Hayashi, H., Kamikuri, S. I., Shiono, M., et al. (2004). Middle Miocene to Pleistocene magneto-biostratigraphy of ODP Sites 1150 and 1151, northwest Pacific: Sedimentation rate and updated regional geological timescale. *Island Arc*, *13*(1), 289–305. https://doi.org/10.1111/j.1440-1738.2003.00426.x

Nagashima, K., Tada, R., Matsui, H., Irino, T., Tani, A., & Toyoda, S. (2007). Orbital- and millennial-scale variations in Asian dust transport path to the Japan Sea. *Palaeogeography, Palaeoclimatology, Palaeoecology*, *247*(1–2), 144–161. https://doi.org/10.1016/j.palaeo.2006.11.027

Nakajima, T., Danhara, T., Iwano, H., & Chinzei, K. (2006). Uplift of the Ou Backbone Range in Northeast Japan at around 10 Ma and its implication for the tectonic evolution of the eastern margin of Asia. *Palaeogeography, Palaeoclimatology, Palaeoecology*, *241*(1), 28–48. https://doi.org/10.1016/j.palaeo.2006.06.009

Nimmergut, A., & Abelmann, A. (2002). Spatial and seasonal changes of radiolarian standingstocks in the sea of Okhotsk. *Deep-Sea Research I*, *49*, 463–493. https://doi.org/10.1016/S0967-0637(01)00074-7

Ohkushi, K., Itaki, T., & Nemoto, N. (2003). Last Glacial-Holocene change in intermediate-water ventilation in the Northwestern Pacific. *Quaternary Science Reviews*, *22*(14), 1477–1484. https://doi.org/10.1016/S0277-3791(03)00082-9

Okazaki, Y., Timmermann, A., Menviel, L., Harada, N., Abe-Ouchi, A., Chikamoto, M., et al. (2010). Deepwater formation in the North Pacific during the last glacial termination. *Science*, *329*(5988), 200–204. https://doi.org/10.1126/science.1190612

Quan, T. M., Wright, J. D., & Falkowski, P. G. (2013). Co-variation of nitrogen isotopes and redox states through glacial-interglacial cycles in the Black Sea. *Geochimica et Cosmochimica Acta*, *112*, 305–320. https://doi.org/10.1016/j.gca.2013.02.029

Rae, J. W. B., Gray, W. R., Wills, R. C. J., Eisenman, I., Fitzhugh, B., Fotheringham, M., et al. (2020). Overturning circulation, nutrient limitation, and warming in the Glacial North Pacific. *Science Advances*, *6*, eabd1654. https://doi.org/10.1126/sciadv.abd1654

Rae, J. W. B., Sarnthein, M., Foster, G. L., Ridgwell, A., Grootes, P. M., & Elliott, T. (2014). Deep water formation in the North Pacific and deglacial CO_2 rise. *Paleoceanography*, *29*(6), 645–667. https://doi.org/10.1002/2013PA002570

Robinson, R. S., Kienast, M., Albuquerque, A. L., Altabet, M., Contreras, S., Rdp, H., et al. (2012). A review of nitrogen isotopic alteration in marine sediments. *Paleoceanography*, *27*(4), 89–108. https://doi.org/10.1029/2012PA00232

Sagayama, T. (2002). Middle Miocene to Pliocene sedimentary basin analysis of vertical movements in Hokkaido, Japan. *Revista Mexicana de Ciencias Geológicas*, *19*(3), 215–225. https://www.redalyc.org/articulo.oa?id=57219308

Sarmiento, J. L., Hughes, T. M. C., Stouffer, R. J., & Manabe, S. (1998). Simulated response of the ocean carbon cycle to anthropogenic climate warming. *Nature*, *393*, 245–249. https://doi.org/10.1038/30455

Schenau, S. J., Prins, M. A., Lange, G. J. D., & Monnin, C. (2001). Barium accumulation in the Arabian Sea: Controls on barite preservation in marine sediments. *Geochimica et Cosmochimica Acta*, *65*(10), 1545–1556. https://doi.org/10.1016/S0016-7037(01)00547-6

Schoepfer, S. D., Shen, J., Wei, H., Tyson, R. V., Ingall, E., & Algeo, T. J. (2015). Total organic carbon, organic phosphorus, and biogenic barium fluxes as proxies for paleomarine productivity. *Earth-Science Reviews*, *149*, 23–52. https://doi.org/10.1016/j.earscirev.2014.08.017

Schubert, C. J., & Calvert, S. E. (2001). Nitrogen and carbon isotopic composition of marine and terrestrial organic matter in Arctic Ocean sediments: Implications for nutrient utilization and organic matter composition. *Deep Sea Research I: Oceanographic Research Papers*, *48*(3), 789–810. https://doi.org/10.1016/S0967-0637(00)00069-8

Shaw, T. A., Baldwin, M., Barnes, E. A., Caballero, R., Garfinkel, C. I., Hwang, Y. T., et al. (2016). Storm track processes and the opposing influences of climate change. *Nature Geoscience*, *9*(9), 656–664. https://doi.org/10.1038/ngeo2783

Shen, X., Wan, S., France-Lanord, C., Clift, P. D., Tada, R., Révillon, S., et al. (2017). History of Asian eolian input to the Sea of Japan since 15 Ma: Links to Tibetan uplift or global cooling? *Earth and Planetary Science Letters*, *474*, 296–308. https://doi.org/10.1016/j.epsl.2017.06.053

Shinjo, R. (1999). Geochemistry of high Mg andesites and the tectonic evolution of the Okinawa Trough–Ryukyu arc system. *Chemical Geology*, *157*, 69–88. https://doi.org/10.1016/S0009-2541(98)00199-5

Sigman, D. M., Karsh, K. L., & Casciotti, K. L. (2009). Ocean process tracers: Nitrogen isotopes in the ocean. In J. H. Steele, K. K. Turekian, & S. A. Thorpe (Eds.), *Encyclopedia of Ocean Sciences* (2nd ed., pp. 40–54). London: Academic Press.

Steinke, S., Groeneveld, J., Johnstone, H., & Rendle-Bühring, R. (2010). East Asian summer monsoon weakening after 7.5 Ma: Evidence from combined planktonic foraminifera Mg/Ca and $\delta^{18}O$ (ODP Site 1146; northern South China Sea). *Palaeogeography, Palaeoclimatology, Palaeoecology*, *289*, 33–43. https://doi.org/10.1016/j.palaeo.2010.02.007

Stüeken, E. E., Kipp, M. A., Koehler, M. C., & Buick, R. (2016). The evolution of Earth's biogeochemical nitrogen cycle. *Earth-Science Reviews*, *160*, 220–239. https://doi.org/10.1016/j.earscirev.2016.07.007

Tada, R. (1994). Paleoceanographic evolution of the Japan Sea. *Palaeogeography, Palaeoclimatology, Palaeoecology*, *108*, 487–508. https://doi.org/10.1016/0031-0182(94)90248-8

Tada, R., Irino, T., Ikehara, K., Karasuda, A., Sugisaki, S., Xuan, C., et al. (2018). High-resolution and high-precision correlation of dark and light layers in the Quaternary hemipelagic sediments of the Japan Sea recovered during IODP Expedition 346. *Progress in Earth and Planetary Science*, *5*, 19. https://doi.org/10.1186/s40645-018-0167-8

Tada, R., Irino, T., & Koizumi, I. (1999). Land-ocean linkages over orbital and millennial timescales recorded in late Quaternary sediments of the Japan Sea. *Paleoceanography*, *14*(2), 236–247. https://doi.org/10.1029/1998PA900016

Tada, R., Murray, R. W., Alvarez Zarikian, C. A., Anderson, W. T., Jr, Bassetti, M. A., Brace, B. J., et al. (2015). Proceedings of the Integrated Ocean drilling Program, Vol. 346, Integrated Ocean Drilling Program, College Station, TX: https://doi.org/10.2204/iodp.proc.346.101

Tamaki, K., Suehiro, K., Allan, J., Ingle, JC., Jr, & Pisciotto, K. A. (1992). Tectonic synthesis and implications of Japan Sea ODP drilling. In K. Tamaki, K. Suyehiro, J. Allan, & M. McWilliams (Eds.), *Proceedings of the ocean drilling Program scientific results*. 127/128 (pp. 1333–1348) Ocean Drilling Program College Station, TX. https://doi.org/10.2973/odp.proc.sr.127128-2.240.1992

Taylor, S. R., & Mclennan, S. M. (1985). *The continental crust: Its composition and evolution*. Oxford: Blackwell Scientific Publications.

Tesdal, J.-E., Galbraith, E., & Kienast, M. (2013). Nitrogen isotopes in bulk marine sediment: Linking seafloor observations with subseafloor records. *Biogeosciences*, *10*(1), 101–118. https://doi.org/10.5194/bg-10-101-2013

Thunell, R. C., Sigman, D. M., Muller-Karger, F., Astor, Y., & Varela, R. (2004). Nitrogen isotope dynamics of the Cariaco Basin, Venezuela. *Global Biogeochemical Cycles*, *18*, GB3001. https://doi.org/10.1029/2003GB002185

Torres, M. E., Brumsack, H. J., Bohrmann, G., & Emeis, K. C. (1996). Barite fronts in continental margin sediments: A new look at barium remobilization in the zone of sulfate reduction and formation of heavy barites in diagenetic fronts. *Chemical Geology*, *127*, 125–139. https://doi.org/10.1016/0009-2541(95)00090-9

Tribovillard, N., Algeo, T. J., Lyons, T., & Riboulleau, A. (2006). Trace metals as paleoredox and paleoproductivity proxies: An update. *Chemical Geology*, *232*, 12–32. https://doi.org/10.1016/j.chemgeo.2006.02.012

Tyson, R. V. (2005). The "productivity versus preservation" controversy: Cause, flaws, and resolution. In N. B. Harries (Ed.), *Deposition of organic-carbon-rich sediments: Models mechanisms, and consequences* (pp. 17–33). SEPM Special Publication. https://doi.org/10.2110/pec.05.82.0017

Waddell, L. M., Hendy, I. L., Moore, T. C., & Lyle, M. W. (2009). Ventilation of the abyssal Southern Ocean during the late Neogene: A new perspective from the subantarctic Pacific. *Paleoceanography*, *24*(3), PA3206. https://doi.org/10.1029/2008PA001661

Wan, S., Clift, P. D., Li, A., Li, T., & Yin, X. (2010). Geochemical records in the South China Sea: Implications for East Asian summer monsoon evolution over the last 20 Ma. *Geological Society, London, Special Publications*, *342*(1), 245–263. https://doi.org/10.1144/SP342.14

Wang, P. X. (1999). Response of Western Pacific marginal seas to glacial cycles: Paleoceanographic and sedimentological features. *Marine Geology*, *156*, 5–39. https://doi.org/10.1016/S0025-3227(98)00172-8

Wan, S., Toucanne, S., Clift, P. D., Zhao, D., Bayon, G., Yu, Z., et al. (2015). Human impact overwhelms long-term climate control of weathering and erosion in southwest China. *Geology*, *43*, 439–442. https://doi.org/10.1130/G36570.1

Warren, B. (1983). Why is no deep water formed in the North Pacific? *Journal of Marine Research*, *41*, 327–347. https://doi.org/10.1357/002224083788520207

Weaver, A. J., Bitz, C. M., Fanning, A. F., & Holland, M. (1999). Thermohaline circulation: High-latitude phenomena and the difference between the Pacific and Atlantic. *Annual Review of Earth and Planetary Sciences*, *27*(1), 231–285. https://doi.org/10.1146/annurev.earth.27.1.231

Whitworth, T., III, Warren, B., Nowlin, W., Jr, Rutz, S., Pillsbury, R., & Moore, M. (1999). On the deep western-boundary current in the Southwest Pacific Basin. *Progress in Oceanography*, *43*(1), 1–54. https://doi.org/10.1016/S0079-6611(99)00005-1

Woodruff, F., & Savin, S. M. (1989). Miocene deepwater oceanography. *Paleoceanography*, *4*(1), 87–140. https://doi.org/10.1029/PA004i001p00087

Yamamoto, M., Naraoka, H., Ishiwatari, R., & Ogihara, S. (2005). Carbon isotope signatures of bacterial 28-norhopanoic acids in Miocene–Pliocene diatomaceous and phosphatic sediments. *Chemical Geology*, *218*, 117–133. https://doi.org/10.1016/j.chemgeo.2005.01.027

Yu, J., Menviel, L., Jin, Z. D., Anderson, R. F., Jian, Z., Piotrowski, A. M., et al. (2020). Last glacial atmospheric CO_2 decline due to widespread Pacific deep water expansion. *Nature Geoscience*, *13*(9), 628–633. https://doi.org/10.1038/s41561-020-0610-5

Zhai, L., Wan, S., Tada, R., Zhao, D., Shi, X., Yin, X., et al. (2020). Links between iron supply from Asian dust and marine productivity in the Japan Sea since four million years ago. *Geological Magazine*, *157*, 818–828. https://doi.org/10.1017/S0016756819000554

Zhang, Y., Pagani, M., Henderiks, J., & Ren, H. (2017). A long history of equatorial deep-water upwelling in the Pacific Ocean. *Earth and Planetary Science Letters*, *467*, 1–9. https://doi.org/10.1016/j.epsl.2017.03.016

Zhang, X., Sigman, D. M., Morel, F. M., & Kraepiel, A. M. (2014). Nitrogen isotope fractionation by alternative nitrogenases and past ocean anoxia. *Proceedings of the National Academy of Sciences of the United States of America*, *111*(13), 4782–4787. https://doi.org/10.1073/pnas.1402976111